Preparation and electrochromic properties of V–Nb mixed-oxide films by evaporation

W. CHEN*, Y. KANEKO and N. KINOMURA
Center for Crystal Science and Technology, Faculty of Engineering, University of Yamanashi, Miyamae 7, Kofu, Yamanashi 400-8155, Japan
(*author for correspondence, fax: +81 55 2208610, e-mail: g01ds006@ccn.yamanashi.ac.jp*)

1. Introduction

Pentoxide vanadium materials, as a counter electrode of WO_3 in electrochromic devices, have been widely investigated using various methods. For example, vanadium oxide films have been prepared by vacuum evaporation [1, 2], sol–gel processes [3], sputtering [4, 5], and chemical vapor deposition [6]. V_2O_5 films prepared by these methods have been found to exhibit less reversibility than tungsten oxide films (beyond 1200 cycles), as reported by Macek et al. [7]. Another drawback of V_2O_5 films is their weaker optical properties [8, 9]. V_2O_5 films darken upon lithium extraction (oxidized state) in the blue and near-U.V. ranges (300–400 nm) and have weak colouration on lithium insertion (reduced state) in the red and near infrared ranges. Due to the effects of such shortcomings, a compromise has to be made between the transmittance range and the maximum transmittance range in designing electrochromical devices with V_2O_5 counter electrodes. To solve these problems, researchers have attempted to minimize the near-infrared colouration of reduced V_2O_5 films by adding dopants such as Ce [10] and Fe [11]. In this study, the electrochromic behaviors of V_2O_5 films modified by Nb_2O_5 were investigated. Niobium was chosen because sputtered Nb_2O_5 films have been observed to exhibit only weak colouration in the visible range and no colouration in the near-infrared range upon lithium insertion [12]. In addition, Nb_2O_5 films have shown high reversibility under voltammetric cycling [13]. In our work, to decrease the deviation in stoichiometry between V–Nb mixed-oxide films and starting materials, V_2O_5 and Nb_2O_5 powders were sintered at 900 °C for 2 h before being evaporated. The compositions of these films were investigated by ICP. Their recharge ability and the cycle reversibility of the Li^+/e^- insertion/extraction process were studied through cyclic voltammetry. Optical properties of lithium ion intercalated/deintercalated films were investigated by *in situ* U.V.–VIS. spectroelectrochemical measurement. The film structures were also studied and characterized by Fourier transform infrared spectroscopy (FTIR), X-ray diffractometry (XRD), and spectrofluorometry.

2. Experimental details

The commercial reagents (99.99%) of V_2O_5 and Nb_2O_5 were used. V_2O_5 powder was mixed with Nb_2O_5 powder with 4, 2, 1, 0.5, and 0.25 molar ratios of vanadium to niobium, respectively. The mixtures were then heated at 900 °C for 2 h. After being ground, they were evaporated onto ITO (indium tin oxide) glass. The vacuum in the chamber was maintained at 5×10^{-4} torr during the evaporation. The formed films were heated in a furnace at 350 °C for 30 min.

The composition of V–Nb mixed-oxide films were analyzed by X-ray photospectroscopy (XPS), and inductively coupled plasma (ICP) after the films were dissolved in an acidic solution. The measured V/Nb molar ratios were close to those of the starting materials. The thickness and surface morphology of the films were investigated by SEM. Cyclic voltammetry was performed at voltages between −2.0 V and +2.0 V relative to Ag/AgCl with a scan rate of 200 mV s^{-1}. *In situ* spectroelectrochemical measurements were carried out using a three-electrode cell with two Pt wires as a counter and a reference electrode installed in a compartment of the scanning spectrophotometer (Shimadzu RF-5300PC). The spectral region used in this work was 300–900 nm. The microstructures of these films were analysed by XRD. The photoluminescence (PL) spectra in the 340–600 nm wavelength region were recorded under 320 nm photoexcitation by a spectrofluorophotometer (Shimadzu UV-3100PC). Fourier transform infrared (FTIR) spectra were recorded by an infrared microscope (Shimadzu AIM-8800) in the 400–4000 cm^{-1} frequency range. The thickness of the films studied was held constant at around 200 nm.

3. Results and discussion

3.1. *Composition and structure of V–Nb mixed-oxide films*

XPS results indicated that vanadium and niobium were at almost their highest oxidation (i.e., V^{5+} and Nb^{5+}) in the V–Nb mixed-oxide films heat-treated at 350 °C for

30 min. These compounds can therefore be expressed as $V_{2-x}Nb_xO_5$. ICP analytical values of V/Nb molar ratios are shown in Table 1. It can be seen that the composition of the films is close to that of the starting materials, and that the composition range of the V–Nb oxide films investigated is $V_{1.6}Nb_{0.4}O_5$ to $V_{0.3}Nb_{0.7}O_5$.

All the V–Nb oxide films heat-treated at 350 °C for 30 min were observed to be noncrystalline based on the XRD pattern (not shown here). They were also observed to be smooth and highly uniform by SEM.

3.2. Characterization of V–Nb oxide films by photospectrometry

Figure 1 shows the infrared absorption spectra of V–Nb oxide films. A sharp absorption peak at 1024 cm^{-1} was observed in the V_2O_5 films. This peak, as pointed out by Frederickson et al. [14], is due to the stretching vibration mode of V=O double bonds. This peak was observed to become weaker and broader and to have a red frequency-shift with increases in the Nb content in V–

Table 1. ICP values for V/Nb molar ratios of V–Nb oxide films

V/Nb molar ratio of starting material	ICP value of V/Nb molar ratio	Deviation /(%)	$V_{2-x}Nb_xO_5$
4	3.8	−5	$V_{1.6}Nb_{0.4}O_5$
2	1.7	−15	$V_{1.3}Nb_{0.7}O_5$
1	1.2	+20	$V_{1.1}Nb_{0.9}O_5$
0.5	0.4	−20	$V_{0.7}Nb_{1.3}O_5$
0.25	0.2	−20	$V_{0.3}Nb_{1.7}O_5$

Nb mixed-oxide films. The peak of the Nb–O stretching at 820 cm^{-1}, as reported by Macek et al. [15], did not appear in the infrared spectra of V–Nb oxide films. These results indicate that V–Nb–O bonds were created and increased in number with increases in the niobium content in V–Nb mixed-oxide films. This conclusion was further illustrated by the photoluminescence (PL) spectra of the films.

Figure 2 shows the photoluminescence (PL) spectra of the V_2O_5 films, the V–Nb oxide films, and the ITO glass. It can be seen that as a film substrate, the ITO glass shows PL peaks in the 450–490 nm wavelength region; it may therefore be concluded that the observed peaks in this wavelength range were caused by the ITO glass. In the PL spectra of V_2O_5 and V–Nb oxide films ($x < 0.9$), a peak near 520 nm can be seen; this peak has been accounted for by Anpo et al. [16] as being due to electron transfer from O^{2-} to V^{5+} and a reverse radiative decay, respectively:

$$(V^{5+}=O^{2-}) \underset{hv'}{\overset{hv}{\rightleftarrows}} (V^{4+}-O^-)$$
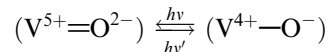
It can also be seen in Figure 2 that the wavelength of the peak near 520 nm does not change with increases in the Nb content in the V–Nb oxide films. V–Nb oxide films with low niobium content include a large number of V=O double bonds. For the V–Nb oxide films with high niobium content ($x \geqslant 0.9$), the peak wavelength near 520 nm had a blue shift with increases in Nb content. It has been clearly indicated that the environmental variation around the V=O double bond can cause a
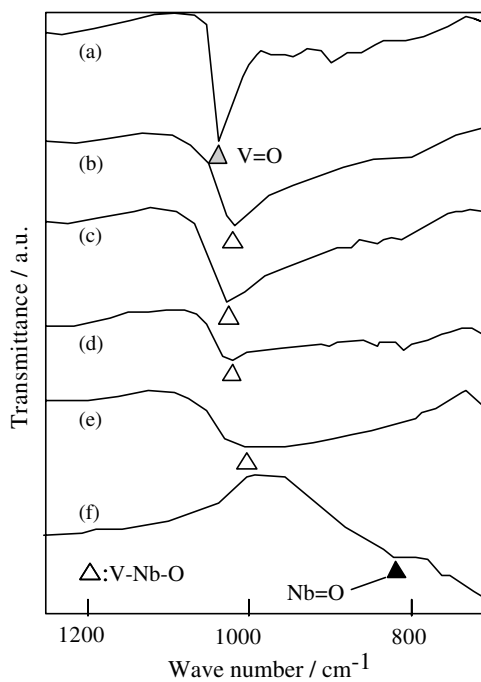

Fig. 1. Infrared absorption spectra of the films heat-treated at 350 °C for 30 min. (a) V_2O_5; (b) $V_{1.6}Nb_{0.4}O_5$; (c) $V_{1.1}Nb_{0.9}O_5$; (d) $V_{0.7}Nb_{1.3}O_5$; (e) $V_{0.3}Nb_{1.7}O_5$; (f) Nb_2O_5.
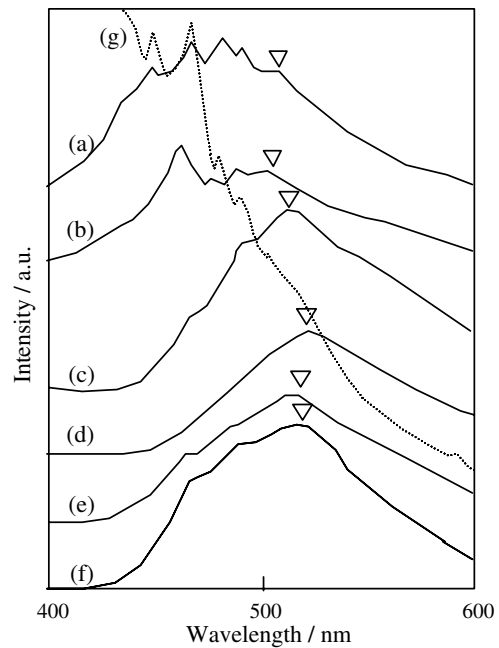

Fig. 2. Change of luminescence spectra depending on the amount of niobium addition in V–Nb oxide films heat-treated at 400 °C for 2 h (thickness approximately 700 nm, upon 320 nm photoexcitation). (a) $V_{0.3}Nb_{1.7}O_5$; (b) $V_{0.7}Nb_{1.3}O_5$; (c) $V_{1.1}Nb_{0.9}O_5$; (d) $V_{1.3}Nb_{0.7}O_5$; (e) $V_{1.6}Nb_{0.4}O_5$; (f) V_2O_5; (g) ITO glass.

PL wavelength shift of this bond. It is therefore likely that the reduction effects of niobium on the V=O double bond lead to a blue shift of the wavelength peak and cause the formation of a V–Nb–O bond.

3.3. EC behavior of the V–Nb oxide films

The reaction of lithium insertion was investigated by cyclic voltammetry performed at voltages between −2.0 V and 2.0 V relative to Ag/AgCl with a scan rate of 200 mV s^{-1}. The $V_{1.6}Nb_{0.4}O_5$ and $V_{0.3}Nb_{1.7}O_5$ films showed higher current density than other V–Nb oxide films. Figure 3 shows typical cyclic voltammograms (CV) of the V_2O_5, Nb_2O_5, $V_{1.6}Nb_{0.4}O_5$ and $V_{0.3}Nb_{1.7}O_5$ films. It can be seen that the $V_{1.6}Nb_{0.4}O_5$ and $V_{0.3}Nb_{1.7}O_5$ films have current densities similar to those of the V_2O_5 film, but higher than those of the Nb_2O_5 film. Moreover, for the cyclic voltammograms of V–Nb oxide films, differences between oxidation and reduction potentials were found to be smaller than for V_2O_5 film, implying that V–Nb oxide films can reduce the amount of electrical energy needed from the battery when used as a counter electrode for WO_3 films in EC device applications.

To check the electrochemical stability of films under voltammetric cycling in Li^+ PC solution, potentials were cycled many times at voltages between 2 V and −2 V relative to Ag/AgCl with a scan rate of 200 mV s^{-1}. After 10 cycles, a large decay was found in the V_2O_5 films. However, decay occurred after 20 cycles in the $V_{1.6}Nb_{0.4}O_5$ films and 100 cycles in the $V_{0.3}Nb_{1.7}O_5$ films. Thus the cyclic stabilities of the $V_{1.6}Nb_{0.4}O_5$ and $V_{0.3}Nb_{1.7}O_5$ films in Li^+ PC solution are apparently superior to those of the V_2O_5 films. In the $V_{1.6}Nb_{0.4}O_5$ and $V_{0.3}Nb_{1.7}O_5$ films, formation of a V–Nb–O bond, as shown by FTIR and PL spectra, may improve the structure of V_2O_5 for Li^+ insertion, parallel to the effects of niobium addition on vanadium bronze [18].

In situ spectroelectrochemistry showed that the colour of V–Nb oxide films heat-treated at 350 °C for 30 min changed depending on the initial state and niobium content of the film. With increases in the niobium content, bleached films changed from yellow to pale yellow, while coloured films changed from dark greenish to dark grayish. Figure 4 shows the typical transmittance spectra of the coloured (−1.8 V) and bleached (1.8 V) $V_{1.6}Nb_{0.4}O_5$, $V_{0.3}Nb_{1.7}O_5$ films and V_2O_5 films in the 300–900 nm range. From this figure, it can be seen that, for the bleached films, the near-U.V. absorption in the V–Nb oxide films is less pronounced than in the V_2O_5 films and decreases in magnitude with increases in the niobium content. In addition, the wavelength of near-U.V. absorption was also observed to shorten with increases in the niobium content. In the coloured state (at −1.8 V), the V–Nb oxide films exhibit a marked increase in transmittance in the 500–900 nm wavelength region as compared to the V_2O_5 films. This phenomenon is similar to the V–Nb oxide films prepared by reactive r.f.-magnetron sputtering [19].
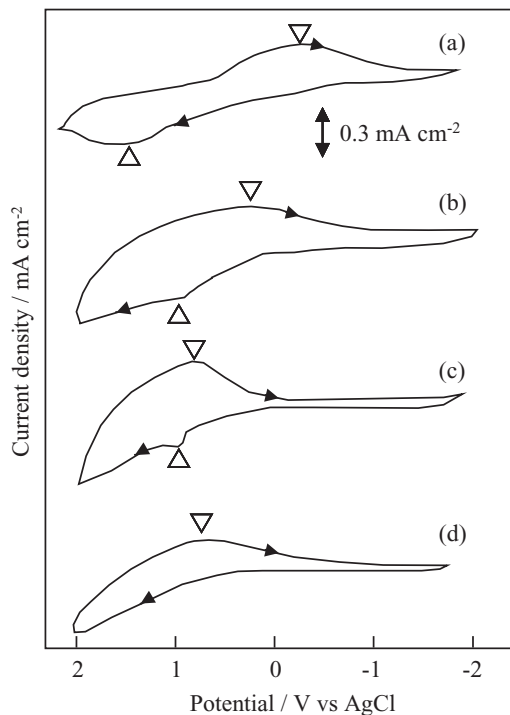

Fig. 3. Effect of niobium addition on the cyclic voltammogram of vanadium oxide films heat-treated at 350 °C for 0.5 h (thickness ∼200 nm) after being recycled ten times. (a) V_2O_5; (b) $V_{1.6}Nb_{0.4}O_5$; (c) $V_{0.3}Nb_{1.7}O_5$; (d) Nb_2O_5.
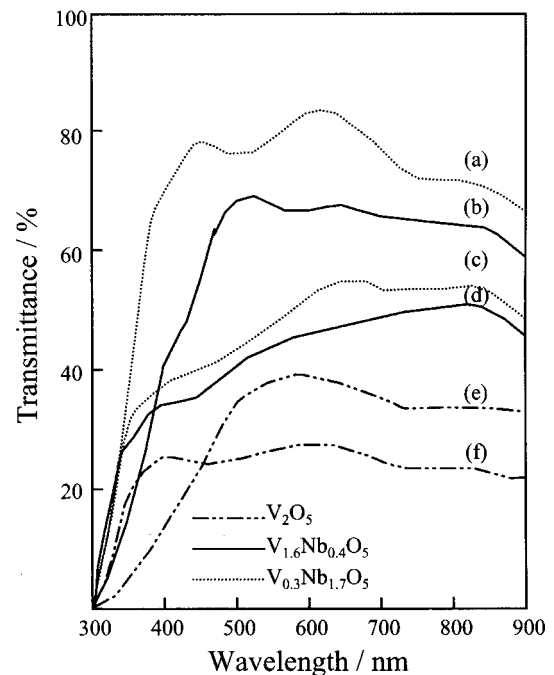

Fig. 4. Effect of niobium addition on the transmittance spectrum of the vanadium oxide films heat-treated at 350 °C for 30 min (thickness ∼200 nm). $V_{0.3}Nb_{1.7}O_5$ films: (a) bleached at 1.8 V, (c) coloured at −1.8 V; $V_{1.6}Nb_{0.4}O_5$ films: (b) bleached at 1.8 V, (d) coloured at −1.8 V; V_2O_5 films: (e) bleached at 1.8 V, (f) coloured at −1.8 V.

Table 2. Average transmittances of the films in the 500–900 nm wavelength

Film	$T/\%$ (Coloured at −1.8 V)	$T/\%$ (Bleached at 1.8 V)
V_2O_5	23.0	32.0
$V_{1.6}Nb_{0.4}O_5$	45.5	66.5
$V_{1.3}Nb_{0.7}O_5$	44.5	63.0
$V_{1.1}Nb_{0.9}O_5$	61.0	78.5
$V_{0.7}Nb_{1.3}O_5$	51.5	80.5
$V_{0.3}Nb_{1.7}O_5$	50.5	74.5

Table 2 shows the average transmittances in the 500–900 nm wavelength region of the V–Nb oxide film in coloured and bleached states. It can be seen that transmittances in the 500–900 nm wavelength region of the V–Nb oxide films are approximately twice as high as those of vanadium oxide films in the coloured and bleached states. Consequently, it can be concluded that the optical properties of V–Nb oxide films are superior to those of V_2O_5 films as a counter electrode for WO_3 films in EC devices.

4. Conclusion

It can be concluded that $V_{1.6}Nb_{0.4}O_5$ and $V_{0.3}Nb_{1.7}O_5$ films show a marked improvement in their recharge ability and cycle reversibility of the Li^+/e^- insertion/extraction process compared with V_2O_5 films. In particular, $V_{0.3}Nb_{1.7}O_5$ films exhibited 10 times better cycling stability than V_2O_5 films. It has been observed that the optical properties of V–Nb oxide films are superior to those of V_2O_5 films as a counter electrode for

WO_3 films in EC devices. FTIR and photoluminescence spectra indicate that V=O double bonds are reduced to V–Nb–O bonds by Nb addition and that the number of V–Nb–O bonds increases with increases in the Nb content.

References

1. Y. Fujita, K. Miyawaki and C. Tatsuyama, *Japanese J. Appl. Phys.* **24** (1985) 1082.
2. Z.S. Guan, J.N. Yao, Y.A. Yang and B.H. Loo, *J. Electroanal. Chem.* **443** (1998) 175.
3. N. Ozer, *Thin Solid Films* **305** (1997) 80.
4. E. Cazzanelli, G. Mariotto, S. Passerini, W.H. Smyrl and A. Gorenstein, *Sol. Energy Mater. Sol. Cells* **56** (1999) 249.
5. M. Ghanashyam Krishna, Y. Debauge and A.K. Bhattacharya, *Thin Solid Films* **312** (1998) 116.
6. D. Barreca, *Chem. Mater.* **12** (2000) 98.
7. M. Macek and B. Orel, *Tr. J. Chem.* **22** (1998) 67.
8. S.F. Cogan, R.D. Rauh, T.D. Plante, N.M. Nguyen and J.D. Westwood, *Electrochem. Society Proc.* (1990) (1902) 99.
9. Y. Shimizu, K. Nagase, N. Miura and N. Yamazoe, *Solid State Ionics* **53–56** (1992) 490.
10. U. Opara Krasovec, B. Orel, A. Surca, N. Bukovec and R. Reisfeld, *Solid State Ionics* **118** (1999) 195.
11. M. Macek, PhD thesis, University of Ljubljana, Slovenia (1997).
12. S.F. Cogan, E.J. Anderson, T.D. Plante and R.D. Rauh, *Proc. Soc. Photo-Opt. Instrum. Eng.* **23** (1985) 562.
13. N. Özer, D-G. Chen and C.M. Lampert, *Thin Solid Films* **277** (1996) 162.
14. L.D. Frederickson and D.M. Hansen, *Anal. Chem.* **35** (1963) 818.
15. M. Macek and B. Orel, *Tr. J. Chem.* **22** (1998) 67.
16. M. Anpo, I. Tanahashi and Y. Kubokawa, *J. Phys. Chem.* **84**(25) (1980) 3441.
17. L. Chen and Y. Kaneko, *Denki Kagaku* **66**(8) (1998) 838.
18. S.F. Cogan, R.D. Rauch, N.M. Nguyen, T.D. Plante and J.D. Westwood, *J. Electrochem. Soc.* **140** (1993) 112.